Virology **297,** 57–67 (2002)
doi:10.1006/viro.2002.1395

Simian Immunodeficiency Virus Encephalitis: Analysis of Envelope Sequences from Individual Brain Multinucleated Giant Cells and Tissue Samples

Elena V. Ryzhova,* Peter Crino,* Linda Shawver,* Susan V. Westmoreland,† Andrew A. Lackner,† and Francisco González-Scarano*,‡,[1]

*Department of Neurology and ‡Department of Microbiology, University of Pennsylvania School of Medicine, Philadelphia, Pennsylvania 19104; and †New England Primate Research Center, Harvard School of Medicine, Southborough, Massachusetts 01772

Received October 16, 2001; accepted January 29, 2002

Simian immunodeficiency virus (SIV)-infected macaques develop an encephalitis (SIVE) that is pathologically virtually indistinguishable from that associated with HIV infection, with multinucleated giant cells (MNGCs) being the principal histopathological manifestation. To dissect SIV variants responsible for MNGC development, we examined the relationships between *env* sequences transcribed in individual MNGCs and those from genomic DNA of brain and spleen tissues. The brain-specific variant found in all brain clones was dominant among the clones from MNGCs, suggesting a role in the formation of giant cells. Furthermore, two additional minor groups of sequences were present in MNGCs. One group consisted of sequences closely related to those from spleen, indicating recent and probably multiple episodes of neuroinvasion. The second group represented clones similar or identical to the initial inoculum. The survival of archival sequences and their activation presumably by the fusion of productively and quiescently infected macrophages/microglia identify the central nervous system as a possible anatomical reservoir for latent infection.

INTRODUCTION

Simian immunodeficiency virus (SIV) infection of macaques is an important animal model for the acquired immunodeficiency syndrome (AIDS) that recapitulates most features of HIV infection, including CNS disease (Desrosiers, 1990; Lackner, 1994). Similar to HIV, the targets for SIV infection *in vivo* and *in vitro* are $CD4^+$ lymphocytes, monocytes, and macrophages (Allen *et al.,* 2000; Lackner *et al.,* 1991a; Veazey *et al.,* 1998, 2000). Moreover, SIV-infected macaques develop an encephalitis that is virtually indistinguishable from that of HIV-infected people, characterized by perivascular aggregates of mononuclear cells and multinucleated giant cells containing viral proteins and genome (Chakrabarti *et al.,* 1991; Lackner *et al.,* 1991b; Ringler *et al.,* 1988; Sharer *et al.,* 1988; Sharma *et al.,* 1992). SIV encephalitis (SIVE) occurs in approximately 25% of SIV-infected macaques (Sasseville and Lackner, 1997; Westmoreland *et al.,* 1998). Furthermore, many of the clinical features of the disease associated with HIV invasion of the CNS, HIV dementia (HIVD), have been replicated in the macaque, including abnormalities of cognition and electrophysiological changes such as prolongation of evoked responses. As with the human disease, these symptoms and findings are ameliorated by antiretroviral therapy (Fox *et al.,* 2000; Gold *et al.,* 1998; Horn *et al.,* 1998; Murray *et al.,* 1992).

Certain viral isolates and specific tropisms are associated with SIVE (Anderson *et al.,* 1993; Kodama *et al.,* 1993; Lane *et al.,* 1995; Mankowski *et al.,* 1997; Prospero-Garsia *et al.,* 1996), paralleling results by some (though not all) investigators of CNS HIV infection, who have suggested that certain HIV envelope sequences are associated with the development of neuropathological changes and neurological disease. Moreover, only macrophage-tropic strains are associated with the development of SIVE in macaques. Regardless of any specific relationship between viral genotypes and disease, there is general agreement that there is some compartmentalization of HIV or SIV within the brain, as viral quasispecies from the central nervous system (CNS) are genetically divergent from those in other organs such as the spleen. This conclusion appears to hold true regardless of the genomic region studied.

These results generate additional questions. First, analysis of proviral DNA, which most of these experiments have undertaken, describes the history of the infection and may not reflect current viral production. Furthermore, the changes may not be reflective of specific adaptation to the CNS, but rather a stochastic phenomenon, perhaps influenced by the relative immunological isolation of the brain. Additionally, the results of PCR amplification from tissue represent the genotype of the majority of quasispecies and may not characterize re-

[1] To whom correspondence and reprint requests should be addressed at Department of Neurology, University of Pennsylvania, 3400 Spruce Street, 3W Gates, Philadelphia, PA 19104-2483. Fax: (215) 662-3362. E-mail: scarano@mail.med.upenn.edu.

0042-6822/02 $35.00

TABLE 1

Summary of the Clinical and Necropsy Data

Necropsy No.	Animal No.	Route of infection	Survival (days)	SAIDS	Neuropathological findings
422	Mm 25-85	Bred with female infected with cloned SIVmac239	≈730	+	Severe MNGC encephalitis
232	Mm 242-91	iv, cloned SIVmac239	1160	+	MNGC encephalitis

gional variation adequately, let alone potential differences in the viruses harbored by differing cell types.

To begin to address some of these issues, we have adapted a technique that analyzes transcription in individual cells (Crino *et al.,* 1996; Tecott *et al.,* 1988) to dissect the expression of SIV genomes within multinucleated giant cells (MNGCs), the hallmark finding in SIVE and HIVE. The findings with this approach demonstrate that there is some microheterogeneity among and within individual MNGCs, setting the stage for more complex regional variability. Additionally, some individual clones were close or identical to the initial inoculum, indicating the survival of archival genomic sequences for relatively long periods of time and their transcription at late stages of the infection.

RESULTS

Specimens

Brain and spleen tissue specimens from two animals (referred to hereafter by their necropsy number), 422 (Mm25-85) and 232 (Mm242-91), with clear evidence of SIVE were used for these studies. The clinical and necropsy data for each animal are summarized in Table 1.

Analysis of *env* genes isolated from tissue samples

To determine whether there is compartmentalization of viral genomes within the CNS, we first amplified the *env* genes from the brains and spleens of the two macaques. Twelve to 16 clones originally obtained from each sample were then tested through *in vitro* transcription–translation reactions. Those clones whose translation products were smaller than approximately 60 kDa (expected size of unglycosylated gp120) were eliminated from further analysis under the assumption that they represented nonfunctional genomes.

The *env* clones obtained from the brains were considerably divergent from the clones amplified from the spleens and clustered in separate lineages according to the phylogenetic reconstruction based on gp160 amino acid sequences (Fig. 1). Furthermore six brain-specific mutations were detected in all brain clones from both cases (Table 2). Three of them, N79S, N198S, and G383R, were located in the gp120, and three changes, L791I, R793G, and T821A, were located in the cytoplasmic portion of the gp41; their potential functional relevance is discussed later. To ensure that the detected mutations were not preexisting in the initial inoculum, we cloned the full-length *env* gene from the parental SIVmac239. Five clones were sequenced and none of them contained the brain-specific mutations. Additionally, about 30% of the clones from both brain and spleen of these

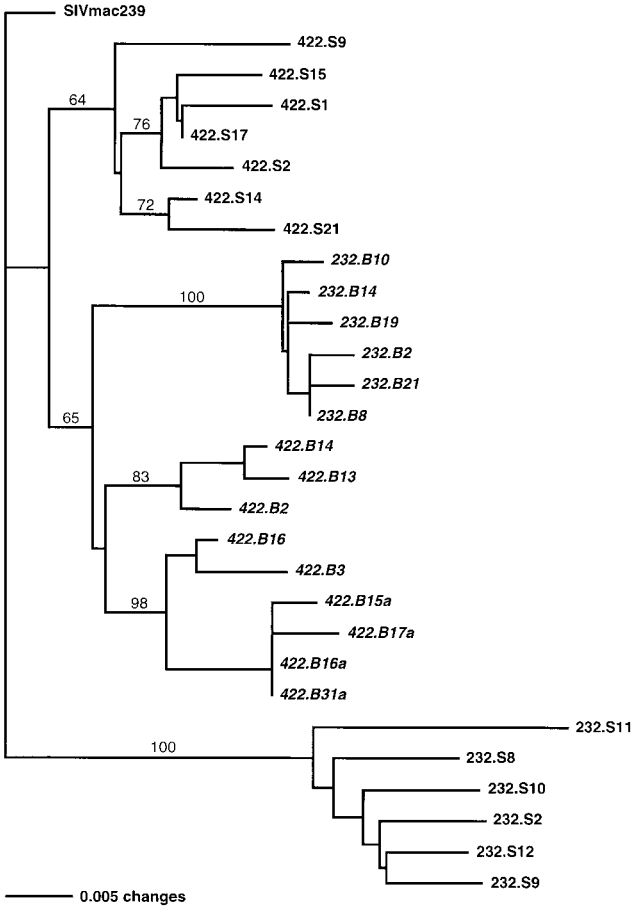

FIG. 1. Phylogenetic comparison of SIV gp160 amino acid sequences in the spleens and brains of two macaques with SIVE. Neighbor-joining trees were constructed as described under Materials and Methods from clones obtained from the spleen (sequences marked with S) or brain (B, italic) of cases 232 and 422. The figure demonstrates compartmentalization of the brain and spleen clones, with the CNS sequences from each animal more closely related to each other than to the spleen sequences. Bootstrap values obtained after 100 resamplings are indicated on the branches.

TABLE 2

Summary of the gp160 Amino Acid Changes Prevailing in the Brain Clones

Necropsy (Macaque No.)	V67M[a]	N79D	K176E	N198S	G383R	L791I	R793G	T821A
422 (Mm25-85)								
Brain	9/9	9/9	9/9	9/9	9/9	9/9	9/9	9/9
Spleen	7/7	0/7	0/7	0/7	0/7	0/7	0/7	0/7
232 (Mm242-91)								
Brain	6/6	6/6	3/6	6/6	6/6	6/6	6/6	6/6
Spleen	0/6	0/6	0/6	0/6	0/6	0/6	0/6	0/6

[a] Amino acid position is numbered according to Regier and Desrosiers (1990).

$SIVE^+$ cases had a premature termination of translation in the gp41 cytoplasmic domain. Similar truncations have been found in a number of SIV isolates, including the well-described neuropathogenic strain SIV/17E-Br (Flaherty *et al.,* 1997). Truncation of the cytoplasmic domain is known to enhance SIV fusogenic capacity (Vzorov and Compans, 1996), sensitivity to neutralization (Vzorov and Compans, 2000), and the ability to replicate in macrophages (Mori *et al.,* 1992) and could therefore play a role in the development of MNGCs.

Amplification of *env* sequences expressed in single multinucleated giant cells

Amplification of the transcribed SIV genes in single multinucleated giant cells is a potential way of determining whether specific genotypes are responsible for the formation of syncytia. Therefore, using a modified technique previously developed for the analysis of neuronal transcription (see Materials and Methods), we analyzed *env* sequences expressed in individual MNGCs, hypothesizing that viral variants directly responsible for this pathology would be prevalent in the fused cells.

For these experiments, pairs of adjacent brain sections were stained with horseradish peroxidase (HRP)-coupled RCA_{120} to identify macrophage/microglial cells for microdissection (Fig. 2). After *in situ* reverse transcription with oligo(dT) primers, MNGCs were dissected from the experimental sections (Fig. 2) and a 1/10 aliquot of the aspirated volume was used in PCR amplification as described under Materials and Methods. The 9062–9455 *env* fragment [numbered according to Regier and Desrosiers (1990)] corresponding to the cytoplasmic domain of the gp41 was chosen for analysis. This region contains three of six brain-specific mutations and includes the sites for premature stop codons detected in a number of clones derived from tissue samples, allowing us to distinguish between brain and spleen quasispecies and to test the potential relevance of truncated Env for syncytia formation.

Our study of viral transcripts from single MNGCs was limited to case 422 (which had severe encephalitis). Although giant cell SIVE was documented in the necropsy of case 232, perhaps because of the lower sensitivity of the staining protocol used for microdissection, we found only one MNGC among the brain sections examined. We were unable to amplify any *env* sequences from this cell. SIV DNA load in brain was quantified using real-time PCR. The absolute copy number of viral DNA was normalized through the use of a GAPDH internal standard. The viral DNA in case 422 was 4.4 ± 1.2 copies of viral DNA per 1000 copies of GAPDH. For case 232 the viral DNA load was approximately twofold lower, 2.15 ± 0.35 copies per 1000 copies of GAPDH. The lower DNA level is likely to reflect the lower virus titer and could be associated with the milder encephalitis and reduced number of MNGCs observed in case 232.

Typical results from an amplification are shown in Fig. 3. An ≈400-bp *env* fragment was produced by RT-PCR from individual MNGCs. To ensure that the template for the PCR was indeed the cDNA derived from the mRNA rather than the proviral DNA, control reactions with primers for GAPDH and β-globin were performed for each cell analyzed. The GAPDH primers were designed to flank the intron-spanning region 3543–4546 and would generate products of either 1 or 0.6 kb in length depending on whether the template used in the reaction was genomic DNA or cDNA, respectively. The β-globin primers were used to detect genomic DNA contamination, since they do not yield any products from cDNA except in erythrocytes. These primers are routinely used in our laboratory and give a reliable yield in the presence of genomic DNA (data not shown).

Only a 600-bp GAPDH fragment was produced in the PCRs using the single-cell template, indicating that PCR synthesis was driven by cDNA copies of spliced mRNA. Similarly, no genomic DNA contamination was detectable in the PCR using primers for the β-globin gene.

To further confirm that the amplified fragments originated from cDNA, we quantified the templates for two MNGCs in real-time PCR. The number of target molecules was $2.5 \times 10^4 \pm 3.8 \times 10^3$ for MNGC1 and $0.9 \times 10^4 \pm 0.1 \times 10^4$ for MNGC2. The amplification plot with a control template showed that the sensitivity of PCR was above 20 copies per reaction (data not shown). Consid-

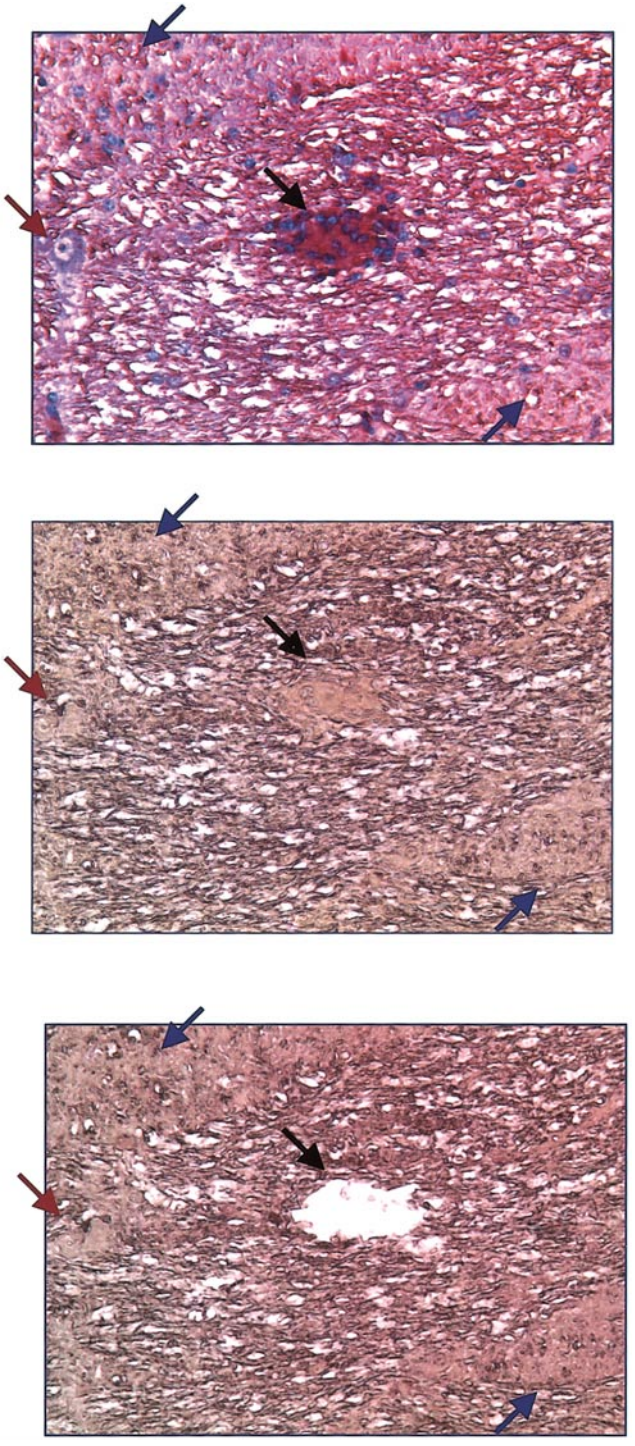

FIG. 2. Microdissection of a single MNGC. Two adjacent sections from case 422 were stained with the lectin *Ricinus communis* agglutinin-2 (RCA_{120}, Sigma) (top and middle). Additionally, one section was stained with Diff-Quick stain to delineate the nuclei and was used as reference for dissection of MNGCs from the experimental section (middle and bottom). Arrows demonstrate the anatomical features of the section (bottom).

ering that only 1/10 aliquot of the sample reverse-transcribed from an individual giant cell was used in PCR, the sensitivity limitation makes amplification from genomic DNA very unlikely.

We analyzed eight MNGCs, and SIV fragments were detected, amplified, and cloned from six giant cells. Sequence analysis of clones corresponding to the gp41 cytoplasmic domain showed that full-length gp41 was expressed in three MNGCs; 1 of 16 clones was found to be truncated for each of two other giant cells and only one MNGC had the *env* population enriched with truncated forms (6/12 clones). The absence of truncated gp41 from some giant cells and their low prevalence in others effectively ruled this out as a necessary phenotype for the formation of MNGCs.

Genetic analysis

Phylogenetic reconstructions were performed with the cytoplasmic domain encoding sequences obtained from mRNA of single MNGCs from case 422 and from genomic DNA of spleen and brain samples from the same animal. Figures 4 and 5 demonstrate the neighbor-joining (N-J) trees based on Jukes–Cantor (J–C) distance measurement. The same groupings were obtained with the maximum-parsimony and maximum-likelihood methods and with various distance estimators for the N-J model, supporting the topology of the presented trees.

The brain and spleen nucleotide sequences formed two separate lineages with bootstrap support of 87 and 57%, correspondingly (Fig. 4A). The relatively low bootstrap confidence level for the splenic branch may be attributed to the significant extent of divergence among the sequences (mean distance $\pm$ SE $=$ 0.0217 $\pm$ 0.0098) and "unfavorable bootstrap conditions" such as unequal rates of change (Hills and Bull, 1993). Sequences from the brain showed close phylogenetic relationships with a

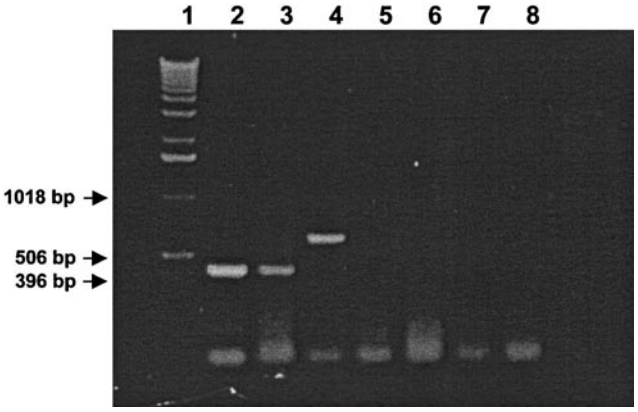

FIG. 3. Amplification of the *env* cytoplasmic domain of individual MNGCs. Individual MNGCs were dissected as demonstrated in Fig. 2, and following RT, the sequences corresponding to the cytoplasmic domain of *env* were amplified, as described under Materials and Methods. Lane 1, DNA ladder; lanes 2 and 3, amplification of cytoplasmic domain from MNGC 1 and MNGC 2, accordingly; lanes 4 and 5, control reactions with cDNA from MNGC 1 and primers for GAPDH and β-globin showed the absence of genomic DNA contamination. The rightmost three lanes are reactions with primers for env, GAPDH, and β-globin, respectively, that did not include template.

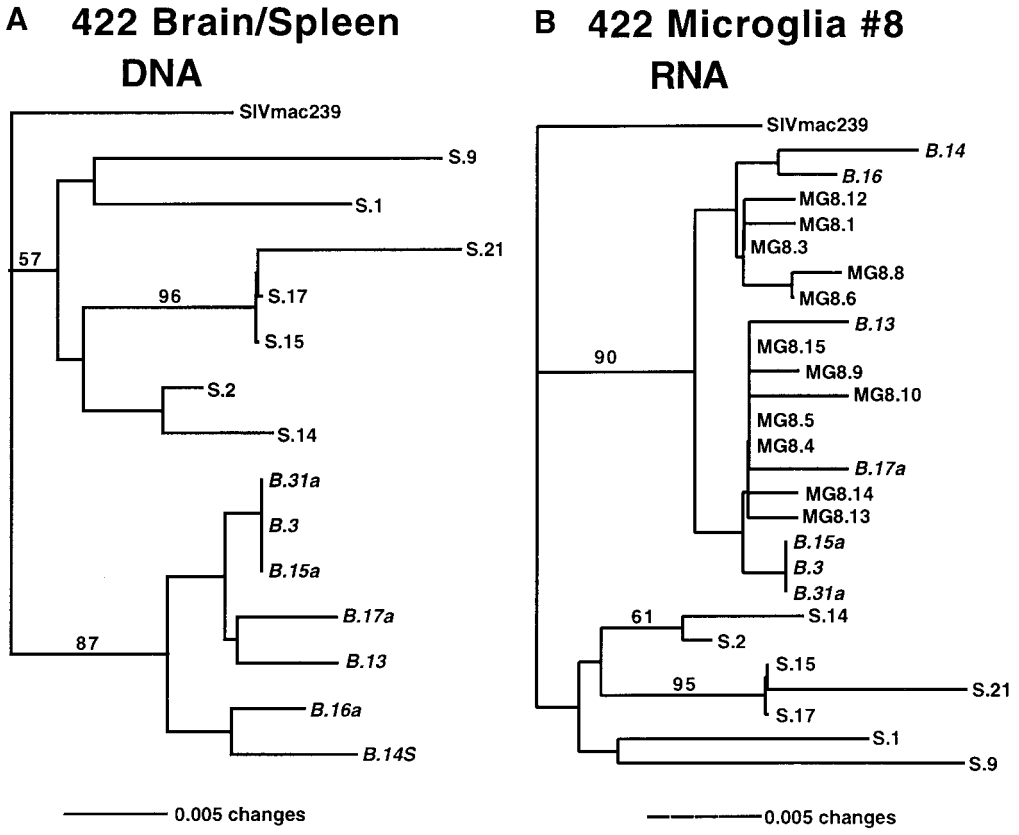

FIG. 4. Phylogenetic analysis of nucleotide sequences from the cytoplasmic domain of the *env* gene. (A) N-J analysis shows the phylogenetic relationships between clones from spleen and brain. (B) Analysis of sequences obtained from single cells shows intermingling of MNGC#8 clones and clones obtained from genomic DNA obtained from brain tissue. These are separate from clones obtained from the spleen of the same animal.

mean pairwise Jukes–Cantor distance of 0.0098 ± 0.0055. Mean pairwise distances between brain and spleen and between brain and SIVmac239 sequences were 0.0296 ± 0.0062 and 0.0255 ± 0.0019, indicating significant divergence of the virus population in the brain from that in the spleen ($P < 0.0001$) and from the ancestor virus ($P < 0.0001$).

We then analyzed the phylogeny of sequences expressed in each of the six individual MNGCs. The clones fit into several patterns, represented in Figs. 4 and 5. In all giant cells there were clones that branched with the brain sequences, as exemplified in Fig. 4B for MNGC#8. In this example, all clones grouped with clones derived from the brain tissue sample with bootstrap support of 90% and they had a brain-specific amino acid signature. The small pairwise distance between brain-derived and single-cell-derived clones (0.0088 ± 0.0041) further confirmed the striking similarity of these sequences.

For other MNGCs, the sequence arrangement was more complex, and two examples are shown in Fig. 5. In these cells (MG#4 and MG#7), there were two additional and interesting patterns. First, along with a number of clones clustering with the brain sequences, several clones grouped with splenic clones. In Fig. 5A clone S.21 from spleen was close to MG4.16, with a bootstrap value of 94% and a pairwise distance of 0.0048. Several clones from MNGC#7 also clustered with spleen taxa and had a common ancestor with the S.9 and S1 clones (Fig. 5B). The detection of viral sequences strictly related to spleen quasispecies suggests recent and, perhaps, multiple episodes of neuroinvasion.

Additionally, and somewhat surprisingly considering that RNA is being analyzed, a number of sequences from each of the six MGNCs analyzed belonged to neither brain nor spleen quasispecies, but rather resembled SIVmac239, the original inoculum (Figs. 5A and 5B). Clone MNGC4.5 showed 100% similarity with the parental virus; the mean pairwise J–C distance between clones 4.12, 4.9, 4.8, 4.7, 4.4, 4.3, and SIVmac239 was as little as 0.0065 ± 0.003 in comparison with distances of 0.0285 ± 0.0057 and 0.0311 ± 0.0071 between these clones and brain and spleen variants. The statistical significance of these differences was confirmed with Student's *t* test ($P < 0.0001$ for both comparisons). Sequences identical or slightly divergent from the parental strain are also illustrated for MNGC#7 (Fig. 5B) and were found in the other MNGCs (data not shown). Since these sequences appeared to not replicate extensively, they are likely to represent latent or defective viruses. Amino acid alignment of representative clones obtained

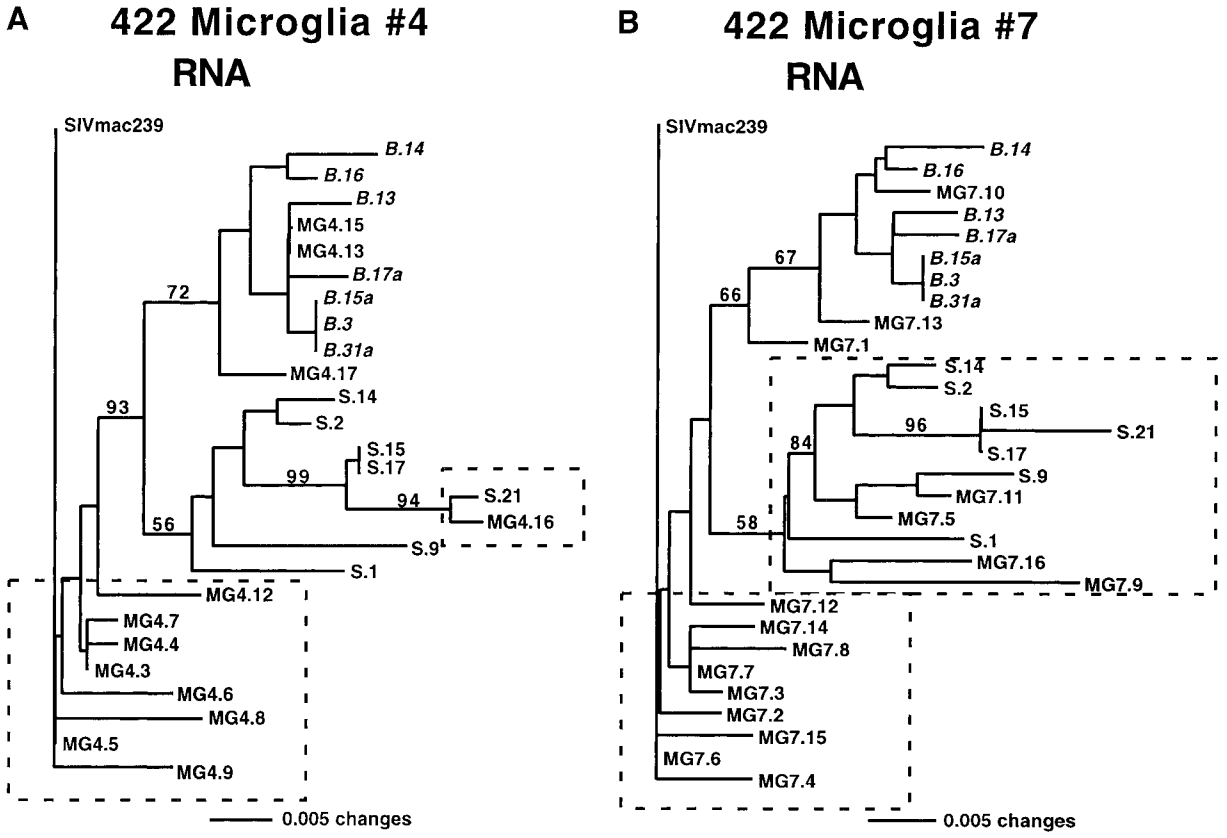

FIG. 5. Phylogenetic analysis of nucleotide sequences from the cytoplasmic domain of *env* gene in two microglia. (A) A clone (MG4.16) obtained from a single MNGC, MNGC#4, is intermingled with spleen clones. Several clones (for example, MG4.3 and MG4.5) demonstrate the preservation of archival sequences. (B) Clones from the spleen segregate with several clones from MNGC#7. As in A, there are sequences that are identical or very close to the initial inoculum.

from MNGC#7 RNA and from brain and spleen genomic DNA is shown in Fig. 6.

It is important to note that the observed distance between clones could overestimate the real distance due to introduction of changes during RT and PCRs. To estimate the enzymatic error, we amplified the 400-bp fragment of the CCR5 gene from brain genomic DNA and single MNGC cDNA and compared the clones with the published rhesus macaque CCR5 sequence (GenBank Accession No. U73739). We detected from 0 to 4 misincorporations (average 0.9 and 1.2 nucleotides/sequence for clones from genomic DNA and a single MNGC, respectively). Subtraction of these errors from the average number of mutations detected in each group of SIV sequences decreased the mutation frequency approximately 10% for clones from brain tissue and approximately 40% for clones from MNGCs. This did not alter the statistical significance of differences between groups of sequences described above, but made the similarity between parental virus and archival sequences even more striking.

Further, to test possible variations in another domain, we analyzed *env* fragment 7553–7868, which includes the V3 encoding region flanked by fragments of C2 and C3. Alignment of the representative clones from each compartment (Fig. 7) illustrates the microheterogeneity found in the V3 loop. Notably, all clones from tissue samples had change L329M, which could therefore be referred to as a host-specific mutation fixed in the virus population at the initial stage of infection. Nevertheless, approximately 20% of the total number of clones from MNGCs showed no changes in this position, in agreement with the findings in the cytoplasmic domain sequences. Overall, the V3 sequences were rather conserved among all brain and spleen clones, with the relative rate of synonymous substitution being twofold higher than that of nonsynonymous substitution. These data suggest that there are functional constraints on sequence variability within V3 and agree with an earlier observation of relatively low variability of V3 in comparison with other SIV *env* hypervariable regions (Overbaugh *et al.,* 1991).

DISCUSSION

We examined the relationship between SIV *env* sequences expressed in individual MNGCs and those obtained from the total genomic DNA of brain and spleen

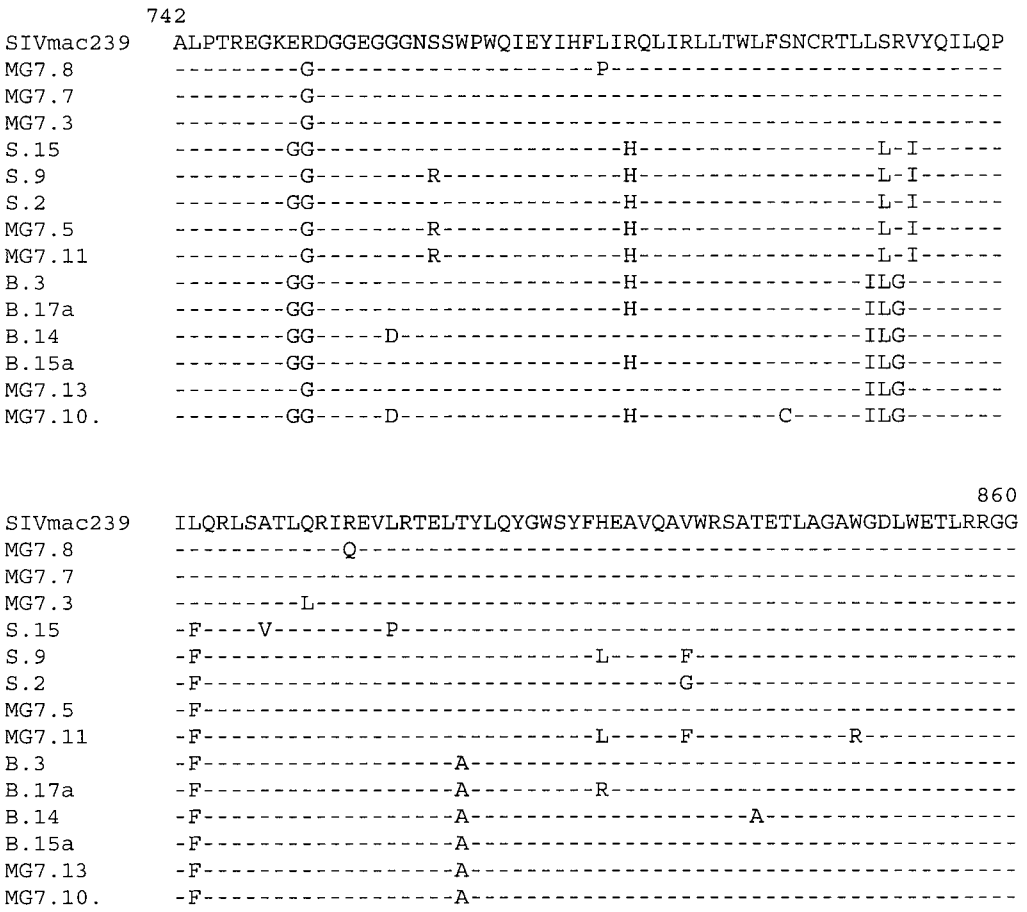

FIG. 6. Amino acid alignment of representative cytoplasmic domain sequences obtained from RNA of MNGC#7 (MG7.) and from genomic DNA of brain (B.) and spleen (S.) tissue samples in comparison with SIVmac239, the original inoculum.

tissue samples. Since MNGC formation is a major histopathological sign of SIVE, this approach would begin to dissect the viral quasispecies that are directly responsible for the development of this very specific CNS pathology.

Phylogenetic analyses of *env* clones obtained from tissue revealed that the brain sequences from two independent SIVE cases grouped together and were significantly divergent from their corresponding splenic clones. Intra- and interanimal comparisons revealed six brain-specific amino acid substitutions not present in the splenic clones, N79S, N198S, G383R, L791I, R793G, and T821A. Change G383R along with V67M and K176E,

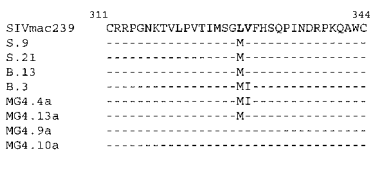

FIG. 7. Alignment of representative V3 sequences amplified from spleen, brain, or MNGC compared with the V3 sequence from the original inoculum SIVmac239. Abbreviations as in Fig. 6. See Results for details.

which were present in the majority of clones from both tissues, has been associated with the acquisition of macrophage tropism (Mori *et al.,* 1992, 2000) and is consistent with the published observation that macrophage tropism is necessary for the development of CNS disease (Flaherty *et al.,* 1997; Kodama *et al.,* 1993; Mankowski *et al.,* 1997). Additional changes N79D and N198S abrogated a potential N-linked glycosylation site in C1 and in the V1/V2 stem, respectively; N198S is of particular interest. First, this type of change has been associated with increased neutralization sensitivity of SIV isolates (Reitter *et al.,* 1998). Second, mutagenesis and an optical biosensor study argued that CD4-gp120 binding induced movement of V1/V2, which in turn leads to greater exposure of the coreceptor binding epitope (Kolchinski *et al.,* 2001; Zhang *et al.,* 2001). It is likely that the loss of the carbohydrate chain in the V1/V2 stem could make the structure more pliable, resulting in alteration of dependence on CD4. Third, N198S and an analogous change for HIV-1, S190R, were found in SIV and HIV isolates obtained by serial passage in microglial cells either *in vivo* or *in vitro* (Lane *et al.,* 1995; Strizki *et al.,* 1996) and are associated with increased fusogenic

capacity in macroglia (Shieh *et al.,* 2000). Taken together these data suggest that N198S could be a possible signature of a microglia-tropic virus variant. The potential function of substitutions found in the gp41 remains unknown.

Although independent evolution of HIV and SIV quasispecies in the brain is well documented (Kodama *et al.,* 1993; Lane *et al.,* 1995; Wong *et al.,* 1997), it is not clear whether the brain genotypes are selected or are the result of genetic drift of a compartmentalized virus population. The convergence of the brain sequences from these SIVE cases into a similar variant argues for adaptive selection.

To determine whether the brain-specific variant found in clones from genomic DNA of whole tissues is also responsible for the development of neuropathology, we analyzed SIV sequences expressed in individual MNGCs, the hallmark of SIVE. A 400-bp fragment encoding the gp41 cytoplasmic domain was chosen for this analysis since it contains 3/6 brain-specific mutations and could therefore provide a fair representation of the brain-specific variant. Alignment and phylogenetic analysis showed that the brain-specific genotype prevailed among the clones from MNGCs, suggesting that it has a major role in the development of syncytia.

However, two additional and potentially important groups of sequences were found in some MNGCs. The first group consists of clones closely related to those from the spleen. The small genetic distance that separates these sequences from their splenic prototypes suggests a recent penetration into the brain from the periphery. The blood–brain barrier is disrupted in SIVE, facilitating the trafficking of SIV-infected monocytes into the brain (Luabeya *et al.,* 2000; Petito and Cash, 1992; Power *et al.,* 1993). This would favor multiple entry events into the brain, particularly at late stages in the disease process (Liu *et al.,* 2000).

The second group, which was more surprising, represented sequences similar or identical to the original inoculum, SIVmac239. In dramatic comparison with the high mutation rates seen in the brain and spleen clones amplified from the entire organ, these clones accumulated few or no changes during 2 years of infection. These sequences probably represent archival viruses that were latent during the bulk of the course of the infection but nevertheless were expressed in the MNGCs.

Our findings led to several interesting conclusions. Latent infection may be established rapidly after primary infection (Chun *et al.,* 1998) and the brain has been considered to be a potential anatomical reservoir. We would argue that the presence and expression of these archival sequences indeed provide evidence that this can occur, and long-lived microglia/brain macrophages appear to be at least one of the cellular reservoirs. SIV could persist in quiescently infected microglia for as long as years (the survival time of the animal studied) and most likely for the life span of these cells. Cell fusion per se may induce activation of latent viruses due to complementation of defective proviral genomes with replication-competent SIV or due to activation of resting microglia/macrophages carrying replication-competent proviruses, explaining their transcription (Inoue *et al.,* 1991).

Although we sequenced as many as 16 clones from the brain tissue, the CNS sequences related to either spleen or parental virus sequences were detected only in the single-cell analysis. The discrepancy between the results obtained by amplification of genomic DNA from the entire tissue sample and from mRNA of single cells may be due to the higher resolution of the latter method, which detects minor sequence populations. Long-term storage of the tissues made expression analysis from the whole tissue sample more difficult due to RNA degradation. An additional advantage of the technique using fixed sections is that it readily allows detection of the viral transcripts even from archival cases because of RNA preservation in these sections.

We would have preferred to compare the *entire* gp160 sequences from single MNGCs to those of whole brain, but perhaps due to a limited amount of the starting material, we could not amplify extensive fragments from single-cell cDNA. However, an additional analysis of the V3 loop, known to be a major determinant of coreceptor choice (Chang *et al.,* 1998; Hu *et al.,* 2000; Isaka *et al.,* 1999; Speck *et al.,* 1997; Trouplin *et al.,* 2001), was performed. The SIV V3 domain shows less variability than the HIV-1 V3 (Overbaugh *et al.,* 1991; Valli and Goudsmit, 1998); sequence differences in SIV gp120 have been shown to be greatest in the V1 and V4 regions followed by V2 and V3 (Valli and Goudsmit, 1998). Consistent with these data, we did not find any significant amino acid variations in this region among spleen and brain clones. Moreover, the rate of synonymous mutations (K_s) detected in these clones exceeded the rate of nonsynonymous mutations (K_a) ($K_s/K_a \approx 2$). In comparison, for the cytoplasmic domain regions from the same clones, $K_s/K_a \approx 1$ (data not shown). This indicates the higher degree of intolerance of amino acid substitutions and the probable role of purifying selection in maintaining the V3 primary structure. Taking into account the recent report that the SIV V3 functions in coreceptor binding identically to that of the HIV-1 V3 (Edinger *et al.,* 2000) we can predict that brain and spleen viruses from this study utilize the same coreceptors.

These results not only reiterate the usefulness of this animal model for pathogenesis studies, but also introduce a technique that can be used to analyze the effects and genetics of lentivirus infection at the single-cell level. With this technology we have now shown that microglial cells can harbor virus for long periods of time serving as an anatomic reservoir for latent SIV infection during the course of this infection. Additionally we believe that the

few sequences in single cells that are closely related to those in the spleen suggest that there are "late" episodes of neuroinvasion, although this interpretation needs to be confirmed with further studies looking at various time points during SAIDS and at more regions within the brain.

MATERIALS AND METHODS

Tissue specimens and brain sections

Archival tissues from two rhesus macaques (*Macaca mulatta*) with SIVE were used in this study. Macaque Mm242-91 (Necropsy 232) was inoculated intravenously with lymphocyte-tropic molecular clone SIVmac239. Macaque Mm25-85 (necropsy 422) was mated with a female that was infected with molecular clone SIVmac239 several months prior to mating. Brain specimens obtained from these animals at necropsy were fixed in 10% formalin, embedded in paraffin, sectioned, and used for histopathological examination and single-cell amplification. Brain and spleen samples from these animals were paraffin embedded, frozen at −70°C, and used as the source of SIV sequences. Brain tissue samples and sections were obtained from the frontal lobe in both cases.

Cloning and analysis of *env* genes from tissue specimens

Genomic DNA from brain and spleen samples was isolated with DNAzol reagent (Gibco BRL) according to the manufacturer's recommendations. Briefly, 25 mg of each tissue was dissolved in 1 ml of reagent and centrifuged for 5 min at 10,000 *g*. Genomic DNA was ethanol precipitated from clarified lysate, removed by spooling onto a pipet tip, and washed two times with 95% ethanol. The pellet was dissolved in 8 mM NaOH. The DNA solution was adjusted to a final pH of 8.0 by the addition of 0.1 M HEPES.

Genomic DNA (0.5–1 μg) was used for amplification of the entire SIV envelope (*env*) gene in a "hot-start" PCR. The reaction was performed with AmpliWax (Perkin–Elmer) according to the manufacturer's instructions in standard PCR buffer in the presence of 2.5 mM $MgCl_2$, a 25 mM concentration of each dNTP, 0.5 U AmpliTaq DNA polymerase (Perkin–Elmer), and 0.1 nM forward (5′GCTCTAGAATGGGATGTCTTGGGAATCAGCTGC3′) and reverse (5′GCTCTAGACCTCACAAGAGAGTGAGCTCAAGCCC3′) primers. *Xba*I and *Bam*HI restriction sites were incorporated into forward and reverse primers, respectively, and were used for cloning into pcDNA3.1 (Invitrogen). In order to clone the full-length *env* gene from parental SIVmac239, CEMx174 cells were infected with an aliquot of the inoculum and cells were collected 7 days after infection. Genomic DNA isolation, *env* gene amplification, and cloning were performed as described above.

In vitro transcription–translation reactions were performed using the two-step STP3 system (Novagen) in which transcription with the T7 RNA polymerase was directly followed by translation in optimized rabbit reticulocyte lysate. Proteins were labeled during synthesis with [^{35}S]methionine (Amersham) and separated in SDS–PAGE. After electrophoresis, the gels were fixed in a mix of isoproanol:water:acetic acid (25:65:10) for 30 min, soaked in Amplify (Amersham) for 30 min, dried, and exposed to X-ray film (Kodak).

Nucleotide sequencing was performed at the core facility operated by the Abramson Institute at the Children's Hospital of Philadelphia. The MacVector 7.0, MEGA1.01, and PAUP 4.0b4a software packages were used to analyze the sequences and to construct phylogenetic trees.

Staining of brain sections

Paraffin-embedded frontal lobe sections were hydrated by sequential incubation in xylene, 5 min ×2, 100% ethanol, 2 min ×2, then 90, 80, and 70% ethanol, for 2 min each. To permeabilize the cells, each section was placed in a methanol solution containing 5% peroxide for 30 min at room temperature. After being washed in water and equilibration with 0.1 M Tris, pH 7.4, each section was stained overnight with the lectin *Ricinus communis* agglutinin-2 (RCA_{120}, Sigma) coupled with horseradish peroxidase (final concentration 10 μg/ml) in 0.1 M Tris, pH 7.4, and 2% FBS. The color was developed with 3-3′diaminobenzidine (Sigma) in the presence of 0.1% peroxide. To identify multinucleated giant cells reference sections were stained with the Diff-Quick Stain Set according to the manufacturer's protocol (Dade International, Inc.).

RT-PCR amplification of SIV *env* from individual cells

Procedures for the synthesis and amplification of cDNA obtained from individual cells have been published previously (Crino *et al.,* 1996; Tecott *et al.,* 1988). Briefly, stained sections were treated with proteinase K and hybridized overnight at room temperature with oligo$(dT)_{15}$ (Promega) in the presence of 5× SSC and 50% formamide. They were then washed in 2× SSC. *In situ* reverse transcription was performed at 37°C for 90 min in a reaction mixture containing 50 mM Tris, pH 8.3, 6 mM $MgCl_2$, 120 mM KCl, 7.5 mM DDT, 250 μM each dNTP, and 100 U AMV reverse transcriptase (RT) (Seikagaku America). Single MNGCs were microdissected from fixed brain sections under light microscopy using a glass Femtotip (Eppendorf) and a joystick micromanipulator. Single cells were aspirated into a second glass microelectrode, transferred to a microfuge tube containing *in situ* RT buffer and AMV RT, and incubated at 40°C for 90 min to ensure cDNA synthesis in the single dissected cell. After phenol/chloroform extraction and ethanol precipitation cDNA–mRNA hybrids were dissolved

in DEPC-treated water and dissociated by heat denaturation (85°C, 5 min, ice, 10 min). Second-strand cDNA synthesis was performed in 0.01 M Tris, pH 7.4, 20 mM KCl, 10 mM $MgCl_2$, 40 mM $(NH_4)_2SO_4$, 2.5 mM each of dNTP, 40 U T4 DNA polymerase (Boehringer Mannheim), 40 U Klenow fragment (Boehringer Mannheim) overnight at +14°C, followed by SI nuclease (Promega) loop excision and blunt ending. After phenol/chloroform extraction and ethanol precipitation, double-stranded cDNA was dissolved in 20 μl of water. Two microliters of cDNA solution was used for PCR amplification of the 3′ fragment of the SIV *env* gene corresponding to the cytoplasmic domain of gp41. Hot-start PCR was conducted under the conditions described above with rTth XL DNA polymerase (Perkin–Elmer). The cytoplasmic domain region was amplified with primers 5′ACCCATATCCAACAGGACCCGG3′ and 5′TGCGAGTATCCATCTTCCACCTC3′; the V3 region was amplified with primers 5′GCCTAAATGTTCTAAGGTGGTGGTC3′ and 5′GGATGTTTGACAATGGTCTGCTTC3′. Representative sequences have been submitted to Genbank (Accession Nos. AY072883–AY072907).

Real-time PCR

Real-time PCR was performed using Molecular Beacon technology (Stratagene) with the primers 5′TCTGCGACCCTACAGAGGATTCG3′ (9316–9349) and 5′CGCGCCCGCAAGAGTCTCTG3′ (9384–9404) and fluorogenic probe 5′GCGAGCTTCCATGAGGCGGTCCAGGCCGCTCGC3′ with reporter (6FAM) dye and quencher dye (DABCYL) attached at the 5′ and 3′ ends, respectively. Quantification of SIV DNA load in the brain DNA was accomplished by normalizing the absolute SIV DNA copy number with a GAPDH internal control for each sample.

ACKNOWLEDGMENTS

This work was supported by PHS Grants MH48958, NS-35743, NS-27405, MH01658, NS-07180, RR00168, NS35732, and RR00150, by the Esther A. and Joseph Klingenstein Fund (PBC), and by the Center for AIDS Research (CFAR) at the University of Pennsylvania. A. Lackner is the recipient of an Elizabeth Glaser Scientist Award. We thank James Hoxie (University of Pennsylvania) for his thoughtful comments.

REFERENCES

Allen, T. M., Connor, D. H., Jing, P., Dzuris, J. L., Mothe, B. R., Vogel, E., Dunphy, T. U., Leibl, M. E., Emerson, C., Wilson, N., Kunstman, K. J., Wang, X., Allison, D. B., Hughes, A. L., Desrosiers, R. C., Altman, J. D., Wolinsky, S. M., Sette, A., and Watkins, D. I. (2000). Tat-specific cytotoxic T lymphocytes select for SIV escape variants during resolution of primary viremia. *Nature* **407,** 386–390.

Anderson, M. G., Hauer, D., Sharma, D. P., Joag, S. V., Narayan, O., Zink, M. C., and Clements, J. E. (1993). Analysis of envelope changes acquired by SIVmac239 during neuroadaptation in rhesus macaques. *Virology* **195,** 616–626.

Chakrabarti, L., Hurtrel, M., Maire, M., Vazeux, R., Dormont, D., Montagnier, L., and Hurtrel, B. (1991). Early viral replication in the brain of SIV-infected rhesus monkeys. *Am. J. Pathol.* **139,** 1273–1280.

Chang, J., Jozwiak, R., Wang, B., Ng, T., Ge, Y. C., Bolton, W., Dwyer, D. E., Randle, C., Osborn, R., Cunningham, A. L., and Saksena, N. K. (1998). Unique HIV type 1 V3 region sequences derived from six different regions of brain: Region-specific evolution within host-determined quasispecies. *AIDS Res. Hum. Retroviruses* **14,** 25–30.

Chun, T-W., Engel, D., Berrey, M. M., Shea, T., Corey, L., and Fauci, A. (1998). Early establishment of a pool of latently infecting, resting T cells during primary HIV-1 infection. *Proc. Natl. Acad. Sci. USA* **95,** 8869–8873.

Crino, P. B., Dichter, M., Trojanowski, J., and Eberwine, J. (1996). Embryonic neuronal markers in tuberous sclerosis: Single cell molecular pathology. *Proc. Natl. Acad. Sci. USA* **93,** 14152–14157.

Desrosiers, R. C. (1990). The simian immunodeficiency viruses. *Annu. Rev. Immunol.* **8,** 557–578.

Edinger, A. L., Ahuja, M., Sung, T., Baxter, K. C., Haggarty, B., Doms, R. W., and Hoxie, J. A. (2000). Characterization and epitope mapping of neutralizing monoclonal antibodies produced by immunization with oligomeric simian immunodeficiency virus envelope protein. *J. Virol.* **74,** 7922–7935.

Flaherty, M. T., Hauer, D. A., Mankowski, J. L., Clements, J. E., and Zink, M. C. (1997). Molecular and biological characterization of neurovirulent molecular clone of simian immunodeficiency virus. *J. Virol.* **71,** 5790–5798.

Fox, H. S., Weed, M. R., Huitron-Resendiz, S., Baig, J., Horn, T. F., Dailey, P. J., Bischofberger, N., and Henriksen, S. J. (2000). Antiviral treatment normalizes neurophysiological but not movement abnormalities in simian immunodeficiency virus-infected monkeys. *J. Clin. Invest.* **106,** 37–45.

Gold, L. H., Fox, H. S., Henriksen, S. J., Buchmeier, M. J., Weed, M. R., Taffe, M. A., Huitron-Resendiz, S., Horn, T. F., and Bloom, F. E. (1998). Longitudinal analysis of behavioral, neurophysiological, viral and immunological effects of SIV infection of rhesus monkeys. *J. Med. Primatol.* **27,** 104–112.

Hills, D. M., and Bull, J. J. (1993). An empirical test of bootstrapping as a method for assessing confidence in phylogenetic analysis. *Syst. Biol.* **42,** 182–192.

Horn, T. F. W., Huitron-Resendiz, S., Weed, M. R., Henriksen, S. J., and Fox, H. S. (1998). Early pathological abnormalities after simian immunodeficiency infection. *Proc. Natl. Acad. Sci. USA* **95,** 15072–15077.

Hu, Q.-X., Trent, J. O., Tomaras, G. D., Wang, Z.-X., Murray, J. L., Conolly, S. M., Novenot, J.-M., Barry, A. P., Greenberg, M. L., and Peiper, S. C. (2000). Identification of Env determinants in V3 that influence the molecular anatomy of CCR5 utilization. *J. Mol. Biol.* **302,** 359–375, doi:10.1006/jmbi.2000.4076.

Inoue, M., Hoxie, J. A., Ramana, R. M. V., Srinivasan, A., and Reddy, E. P. (1991). Mechanisms associated with the generation of biologically active human immunodeficiency virus type 1 particles from defective proviruses. *Proc. Natl. Acad. Sci. USA* **88,** 2278–2282.

Isaka, Y., Sato, A., Miki, S., Kawauchi, S., Sakaida, H., Hori, T., Uchiayama, T., Adachi, A., Hayami, M., Fujiwara, T., and Yoshie, O. (1999). Small amino acid changes in the V3 loop of human immunodeficiency virus type 2 determines the coreceptor usage for CXCR4 and CCR5. *Virology* **264,** 327–243, doi:10.1006/viro.1999.0006.

Kodama, T., Mori, K., Kawahara, T., Ringler, D. J., and Desrosiers, R. C. (1993). Analysis of simian immunodeficiency virus sequence variation in tissues of rhesus macaques with simian AIDS. *J. Virol.* **67,** 6522–6534.

Kolchinsky, P., Kiprilov, E., Bartley, P., Rubenstein, R., and Sodroski, J. (2001). Loss of a single L-linked glycan allows CD4-independent human immunodeficiency virus type 1 infection by altering the position of the gp120 V1/V2 variable loops. *J. Virol.* **75,** 3435–3443.

Lackner, A. A. (1994). Pathology of simian immunodeficiency virus induced disease. *In* "Current Topics in Microbiology and Immunology: Simian Immunodeficiency Virus" (R. C. Desrosiers and N. Letvin, Eds.), pp. 35–64. Springer Verlag, Berlin.

Lackner, A. A., Dandekar, S., and Gardner, M. B. (1991a). Neurobiology

of simian and feline immunodeficiency virus infections. *Brain Pathol.* **1,** 201–212.

Lackner, A. A., Smith, M. O., Munn, R. J., Martfeld, D. J., Gardner, M. B., Marx, P. A., and Dandekar, S. (1991b). Localization of simian immunodeficiency virus in the central nervous system of rhesus monkeys. *Am. J. Pathol.* **139,** 609–621.

Lane, T. E., Buchmeier, M. J., Watry, D. D., Jakubowski, D. B., and Fox, H. S. (1995). Serial passage of microglial SIV results in selection of homogeneous *env* quasispecies in the brain. *Virology* **212,** 458–465.

Liu, Y., Tang, X. P., McArthur, J. C., Scott, J., and Gartner, S. (2000). Analysis of human immunodeficiency virus type 1 gp160 sequences from a patient with HIV dementia: Evidence for monocyte trafficking into brain. *J. Neurovirol.* **6**(Suppl. 1), S70–S81.

Luabeya, M., Dallasta, L. M., Achim, C. L., Pauza, C. D., and Hamilton, R. L. (2000). Blood–brain barrier disruption in simian immunodeficiency virus encephalitis. *Neuropathol. Appl. Neurobiol.* **26,** 454–462.

Mankowski, J. L., Flaherty, M. T., Spelman, J. P., Hauer, D. A., Didier, P. J., Amedee, A. M., Murphey-Corb, M., Kirstein, L. M., Munos, A., Clements, J. E., and Zink, M. C. (1997). Pathogenesis of simian immunodeficiency virus encephalitis: Viral determinants of neurovirulence. *J. Virol.* **71,** 6055–6060.

Mori, K., Ringler, D. J., Kodama, T., and Desrosiers, R. C. (1992). Complex determinants of macrophage tropism in Env of simian immunodeficiency virus. *J. Virol.* **66,** 2067–2075.

Mori, K., Rosenzweig, M., and Desrosiers, R. (2000). Mechanisms for adaptation of simian immunodeficiency virus to replicate in alveolar macrophages. *J. Virol.* **74,** 10852–10859.

Murray, E. A., Raussch, D. M., Lendvay, J., Sharer, L. R., and Eiden, L. (1992). Cognitive and motor impairments associated with SIV infection in rhesus monkeys. *Science* **255,** 1246–1249.

Overbaugh, L., Rudensey, L. M., Papenhausen, M. D., Beneviste, R. E., and Morton, W. R. (1991). Variation in simian immunodeficiency virus Env is confined to V1 and V4 during progression to simian AIDS. *J. Virol.* **65,** 7025–7031.

Petito, C. K., and Cash, K. S. (1992). Blood–brain barrier abnormalities in the aquired immunodeficiency syndrome: Immunohistochemical localization of serum proteins in postmortem brain. *Ann. Neurol.* **32,** 658–666.

Power, C., Kong, P. A., Crawford, T. O., Wesselingh, S., Glass, J. D., MacArthur, J. C., and Trapp, B. D. (1993). Cerebral white matter changes in acquired immunodeficiency syndrome dementia: Alteration of the blood–brain barrier. *Ann. Neurol.* **34,** 339–350.

Prospero-Garsia, O., Gold, L. H., Fox, H. S., Polis, I., Koob, G. F., Bloom, F. E., and Henriksen, S. J. (1996). Microglia-passaged simian immunodeficiency virus induces neurophysiological abnormalities in monkeys. *Proc. Natl. Acad. Sci. USA* **93,** 14158–14163.

Regier, D. A., and Desrosiers, R. C. (1990). The complete nucleotide sequence of a pathogenetic molecular clone of simian immunodeficiency virus. *AIDS Res. Hum. Retroviruses* **6,** 1221–1231.

Reitter, J. N., Means, R. E., and Desrosiers, R. C. (1998). A role for carbohydrates in immune evasion in AIDS. *Nat. Med.* **4,** 679–684.

Ringler, D. J., Hunt, R. D., Desrosiers, R. C., Daniel, M. D., Chalifoux, L. V., and King, N. W. (1988). Simian immunodeficiency virus-induced meningoencephalitis: Natural history and retrospective study. *Ann. Neurol.* **23**(Suppl.), S101–S107.

Sasseville, V. G., and Lackner, A. (1997). Neuropathogenesis of simian immunodeficiency virus infection in macaque monkeys. *J. Neurovirol.* **3,** 1–9.

Sharer, L. R., Baskin, G. B., Cho, E.-S., Murphey-Corb, M., Blumberg, B. M., and Epstein, L. G. (1988). Comparison of simian immunodeficiency virus and human immunodeficiency virus encephalitis in the immature host. *Ann. Neurol.* **23**(Suppl.), S108–S112.

Sharma, D. P., Zink, M. C., Anderson, M., Adams, R., Clements, J. E., Joag, S. V., and Narayan, O. (1992). Derivation of neurotropic simian immunodeficiency virus from exclusively lymphocytotropic parental virus: Pathogenesis of infection in macaques. *J. Virol.* **66,** 3550–3556.

Shieh, J. T. C., Martin, J., Baltuch, G., Malim, M. H., and González-Scarano, F. (2000). Determinants of syncytium formation in microglia by human immunodeficiency virus type 1: Role of the V1/V2 domains. *J. Virol.* **74,** 693–701.

Speck, R. F., Wehrly, K., Platt, E. J., Atchison, R. E., Charo, I. F., Kabat, D., Chesebro, B., and Goldsmith, M. A. (1997). Selective employment of chemokine receptor as human immunodeficiency virus type 1 coreceptors determine by individual amino acids within the envelope V3 loop. *J. Virol.* **71,** 7136–7139.

Strizki, J. M., Albright, A. V., Sheng, H., O'Connor, M., Perrin, L., and González-Scarano, F. (1996). Infection of primary human microglia and monocyte-derived macrophages with human immunodeficiency virus type 1 isolates: Evidence of differential tropism. *J. Virol.* **70,** 7654–7662.

Tecott, L. H., Barchas, J. D., and Eberwine, J. H. (1988). In situ transcription: Specific synthesis of complementary DNA in fixed tissue sections. *Science* **240,** 1661–1664.

Trouplin, V., Salvatori, F., Cappello, F., Obry, V., Brelot, A., Heveker, N., Alizon, M., Scarlatti, G., Clavel, F., and Mammano, F. (2001). Determination of coreceptor usage of human immunodeficiency virus type 1 from patient plasma samples by using a recombinant phenotypic assay. *J. Virol.* **75,** 251–259.

Valli, P. J. S., and Goudsmit, J. (1998). Structured-tree topology and adaptive evolution of the simian immunodeficiency virus SIVsm envelope during serial passage in rhesus macaques according to likelihood mapping and quartet puzzling. *J. Virol.* **72,** 3673–3683.

Veazey, R. S., DeMaria, M., Chalifoux, L. V., Shvetz, D. E., Pauley, D. R., Khight, H. L., Rosenzweig, M., Johnson, R. P., Desrosiers, R. C., and Lackner, A. A. (1998). Gastrointestinal tract as a major site of $CD4^+$ T cell depletion and viral replication in SIV infection. *Science* **280,** 427–431.

Veazey, R. S., Mansfield, K. G., Tham, I. C., Carville, A. C., Shvetz, D. E., Forand, A. E., and Lackner, A. A. (2000). Dynamics of CCR5 expression by $CD4^+$ T cells in lymphoid tissues during simian immunodeficiency virus infection. *J. Virol.* **74,** 11001–11007.

Vzorov, A. N., and Compans, R. W. (1996). Assembly and release of SIV *env* protein with full-length or truncated cytoplasmic domains. *Virology* **221,** 22–33, doi:10.1006/viro.1996.0349.

Vzorov, V., and Compans, R. W. (2000). Effect of the cytoplasmic domain of the simian immunodeficiency virus envelope protein on the incorporation of heterologous *env*elope proteins and sensitivity to neutralization. *J. Virol.* **74,** 8219–8225.

Westmoreland, S. V., Halpern, E., and Lackner, A. A. (1998). Simian immunodeficiency virus encephalitis in rhesus macaques is associated with rapid disease progression. *J. Neurovirol.* **4,** 260–268.

Wong, J. K., Ignacio, C. C., Torrianni, F., Havlir, D., Fitch, N. J. S., and Richman, D. D. (1997). In vivo compartmentalization of human immunodeficiency virus: Evidence from the examination of pol sequences from autopsy tissues. *J. Virol.* **71,** 2059–2071.

Zhang, W., Godillot, A. P., Wyatt, R., Sodroski, J., and Chaiken, I. (2001). Antibody 17b binding at the coreceptor site weakens the kinetics the interaction of envelope glycoprotein gp120 with CD4. *Biochemistry* **40,** 1662–1670.